

Contents lists available at ScienceDirect

Carbon Trends

journal homepage: www.elsevier.com/locate/cartre



Effects of laser power and substrate on the Raman shift of carbon-nanotube papers



Fuqian Yang*, Shanshan Wang, Yulin Zhang

Materials Program, Department of Chemical and Materials Engineering, University of Kentucky, Lexington, KY 40506, United States

ARTICLE INFO

Article history: Received 6 October 2020 Revised 10 November 2020 Accepted 11 November 2020

Keywords: Carbon-nanotube papers Raman shift Laser power Thermoelastic deformation

ABSTRACT

The progress in the fabrication of carbon-nanotube-based structures has made it possible to use Raman spectroscopy to measure the deformation states of carbon nanotubes and abutting materials. In this work, we investigate the effects of laser power and surrounding materials on the Raman shift of carbon-nanotube (CNT) papers for the laser intensity in a range of 0.071 to 1.415 kW/mm² without action of mechanical loading. Two different configurations of the CNT papers are used in the Raman measurement; one uses a suspended CNT paper, and the other places a CNT paper on a glass or aluminum substrate. The experimental results reveal that there exist combinational effects of the laser power and abutting materials on the changes of the wavenumbers of the D, G and G' bands of the CNT papers. We derive an analytical relation between the strain components, temperature and the change of the wavenumber of the Raman peak, which yields a proportional relationship between the change of the wavenumber of the Raman peak and the laser power. Such a relationship is supported by the experimental results.

© 2020 The Author(s). Published by Elsevier Ltd. This is an open access article under the CC BY-NC-ND license (http://creativecommons.org/licenses/by-nc-nd/4.0/)

1. Introduction

Raman spectroscopy, a non-destructive technique for chemical analysis, has been extensively used to study structural changes under a variety of external stimuli [1]. In the heart of Raman spectroscopy is the Raman scattering due to the interaction between electromagnetic wave and chemical bonds of materials. The change in the relative distance and orientation between atoms due to local deformation, such as stretch, twist, etc., can cause the change in chemical bond strength of materials, leading to the change in the interaction between electromagnetic wave and the chemical bonds of materials and the shift in the Raman peak positions from the change in the frequencies of Raman-induced phonons and/or molecular vibrations [2].

In general, the deformation state of a material is dependent on temperature and stresses. Using the principle for deformation-induced Raman shift, Raman spectroscopy has been used in the stress analysis of semiconductors [3, 4], carbon nanotubes [5, 6] and graphene [7–9] and the temperature measurement [10, 11]. Huang et al. [12] studied the temperature dependence of the Raman spectra of carbon nanotubes (CNTs), active carbon and highly ordered pyrolytic graphite with different excitation powers and ob-

* Corresponding author. E-mail address: fuqian.yang@uky.edu (F. Yang). served red shift of the Raman peaks with the increase of temperature. They did not analyze the effects of laser power on the shift of the Raman peaks and provide the substrate information. Using laser intensity in a range of 1 to 100% of 10⁵ W/cm², Zhang et al. [13] studied the effect of laser intensity on the Raman spectra of single-wall carbon nanotubes (SWCNTs) under the laser irradiation of 514.5 nm in wavelength. They found that increasing the laser intensity caused red shift of the Raman peak of G band, while they did not provide the information of substrate. Steiner et al. [14] observed red shifts of both G+ and G- bands of CNTs in CNT-based field-effect transistors with electrical power (the phonon temperature is a linearly increasing function of electrical power), suggesting the temperature effect on the shift of the Raman peak. Sharma et al. [15] studied temperature-dependent Raman spectra for temperature in a range of 173 to 723 K. Their results suggest that the width for the G band of MWCNTs is relatively independent of temperature. Using Raman excitation spectroscopy, Steiner et al. [16] compared the Raman spectrum of suspended SWCNTs with the Raman spectrum of the SWCNTs on SiO2-substrate for laser intensity in a range of 1.5 to 180 kW/cm². They found that the wavelength of the Raman peak corresponding to G band was relatively independent of the laser intensity for the SWCNTs on SiO2substrate and decreased with the increase in the laser intensity for the suspended SWCNTs. They commented the laser-induced heating without providing the reason for the shift of the Raman peak.

Fig. 1. Schematic of two configurations used in the Raman measurement: (a) a suspended CNT paper, and (b) a CNT paper supported on a solid substrate.

Li et al. [17] found that the tension of CNT-papers led to slight red shift of G' band. All these results suggest that there exist the effects of temperature and deformation on the characteristics of the Raman spectrum of CNTs and CNT-based structures. It is of great importance to study if there exist the dual effects of laser irradiation on the characteristics of the Raman spectrum of CNTs.

Considering the potential of CNTs as electronic, photonic and structural materials, we study the effect of laser power on the Raman shift of CNT-papers. Two different configurations, as shown in Fig. 1, are used in this work; the first one uses a suspended CNT paper, and the second one places a CNT paper on a solid substrate. To examine the possible effect of heat conduction, we use aluminum and glass substrates to support the CNT paper. Note that the thermal conductivity of aluminum is much larger than sodalime glass. The variations of the three bands of D, G and G' with laser power (intensity) are presented.

2. Experimental detail

The CNT papers used in this work were from Suzhou Institute of Nano-tech and Nano-bionics, (Suzhou, China). The CNT papers consisted of disordered carbon nanotubes in non-woven form [18], and the thickness of the CNT papers was ~8 μ m. Glass slides of 75 mm in length and 25 mm in width were from VWR International (Radnor, PA), and a large plate of aluminum alloy (AA6061) were from Alfa Aesar (Ward hill, MA). Aluminum plates of $75 \times 35 \times 6.35$ mm³ in dimensions were cut from the large aluminum plate. Both the glass and aluminum plates were cleaned in acetone (ACS reagent, $\geq 99.5\%$) ultrasonically and rinsed in deionized (DI) water for 10 min, sequentially. The plates were then placed in an oven to evaporate the residual of water. prior to the placement of a CNT paper on the surface of the plates.

Two different configurations, as shown in Fig. 1, were used for the Raman measurement. The first one (Fig. 1a) used a suspended CNT paper, which was supported simply on edges; the second one (Fig. 1b) placed a CNT paper on the surface of either glass or aluminum plate. The Raman spectrum of the CNT papers was collected on a DXR Raman Microscope (Thermo Scientific, DXR3) with a laser wavelength of 532 nm, spectral resolution of 2 cm⁻¹ FWHW (full width at half maximum), in-plane spatial resolution of 1 μ m and depth resolution of 2 μ m. Thermo Scientific OMNICTM software was used for instrument control and data acquisition. The Raman measurement for the same laser power (intensity) was repeated five times at five different positions, which were selected randomly. Five different laser powers of 0.5, 1, 2, 5 and 10 mW were used to analyze the effect of laser power (intensity) on the Raman shift. The size of laser spot was $\sim 3 \mu m$, and the peak laser intensities corresponding to the laser powers of 0.5, 1, 2, 5 and 10 mW were 0.071, 0.142, 0.283, 0.708, and 1.415 kW/mm², respectively. Note that there were no structural damages to the CNT papers under the laser irradiation with the laser intensity equal to or less than 1.415 kW/mm².

The structure of the CNT papers was analyzed on a scanning electron microscope (SEM) (Hitachi S4300, Japan) and a transmis-

sion electron microscope (TEM) (Talos F200X, ThermoFisher Scientific, Waltham, MA).

3. Results

Fig. 2 shows SEM images of the CNT papers under different magnifications. It is evident that long and smooth CNTs of different sizes/radii are randomly entangled together and in contact with adjacent CNTs to form a mat-like structure. There are empty spaces (pores) around the CNTs, and some CNTs are "welded" together to form "knots". The intimate contact between the CNTs warrants that the CNT papers are a good thermal conductor.

Fig. 3 depicts TEM and HRTEM images of the CNTs in a CNT paper. It is evident that the CNTs are presented in a tubular-like structure with a hollow core (Fig. 3a). There are Fe nanoparticles, which are randomly distributed over the CNTs (Fig. 3a and b). The Fe nanoparticles were the catalyst used in the production of the CNTs. The HRTEM image (Fig. 3c) reveals that there are very few defects in the CNTs and the CNTs exhibit a high degree of crystallinity. The d-spacing is 0.33 nm, representing the (002) plane of graphitic structure.

Fig. 4 presents the Raman spectra of the CNT papers with and without solid substrate for different laser powers. There are three peaks presented in the wavenumber range of 1000 to 3000 cm⁻¹, which correspond to D (~1350 cm⁻¹), G (~1583 cm⁻¹) and G' (~2692 cm⁻¹) bands, respectively. To illustrate possible shift of the Raman peaks with the laser power/intensity used in the Raman measurement, we replot the Raman spectra of individual G and G' bands of the CNT papers (Fig. 4-a2-3, 4-b2-3 and c2-3). It is evident that there indeed exists the red shift of the Raman peaks with the laser power/intensity. That is to say, the wavenumbers of the corresponding Raman peaks are likely dependent on the laser power/intensity used in the Raman measurement.

From Fig. 4, we determine the wavenumbers of the corresponding Raman peaks. Fig. 5 shows the variations of the wavenumbers of D, G and G' bands with the laser power. For the suspended CNT papers, the laser irradiation with the laser power equal to or less than 2 mW has statistically no effect on the wavenumbers of all the three Raman peaks. However, the wavenumbers of all the three Raman peaks decrease with the increase of the laser power for the laser power in the range of 2 to 10 mW. For the CNT papers on glass slide, the wavenumber for the D band is statistically independent of the laser power for the laser power in the range of 0.5 to 10 mW. Both the wavenumbers of the G and G' bands decrease with the increase of the laser power for the laser power in the range of 0.5 to 10 mW. For the CNT papers on aluminum plate, the laser irradiation with the power equal to or less than 2 mW has statistically no effect on the wavenumbers of the D and G bands. However, the wavenumbers of both the D and G bands decrease with the increase of the laser power for the laser power in the range of 2 to 10 mW. The wavenumber of the G' band exhibits a slightly different trend from those of both the D and G bands and decreases with the increase of the laser power for the laser power in the range of 0.5 to 10 mW. Also, the wavenumber of the D band

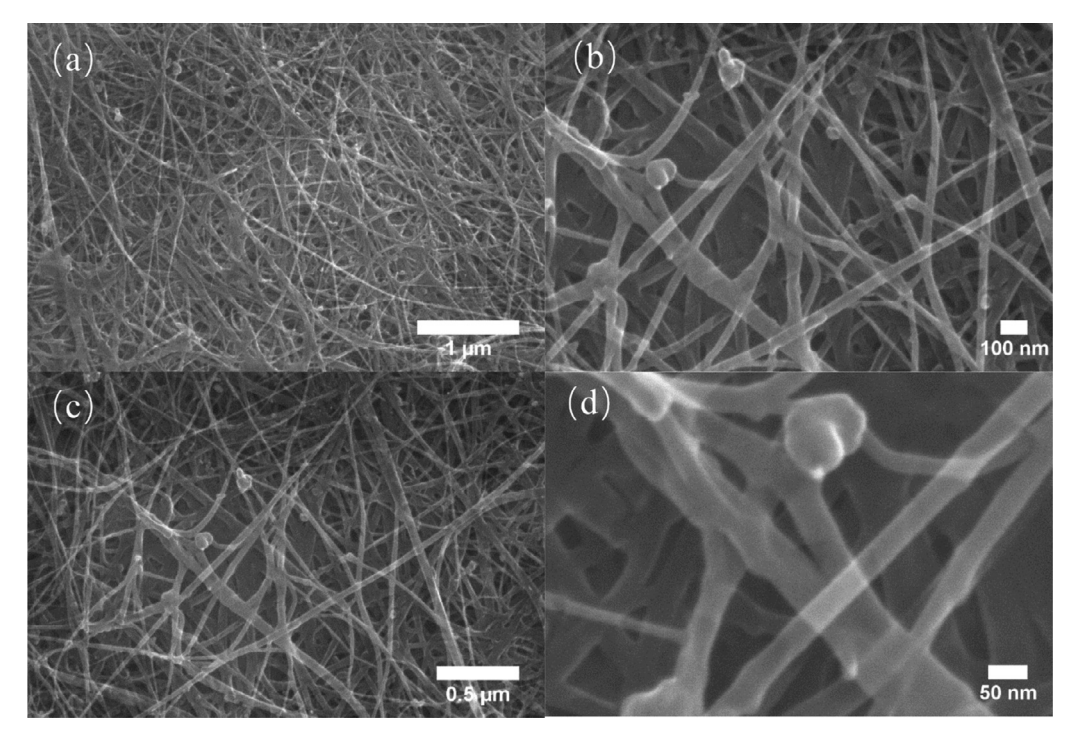


Fig. 2. SEM images of the CNT papers under different magnifications.

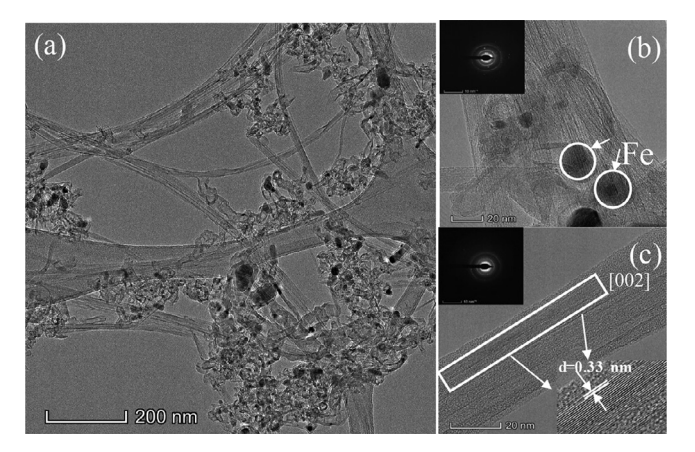


Fig. 3. TEM and HRTEM images of CNTs in a CNT paper: (a) TEM image, (b) HRTEM image with presence of Fe nanoparticles, and (c) d-spacing of 0.33 nm

is dependent on the substrate (air, glass and aluminum) with the largest wavenumber for the suspended CNT papers and the smallest wavenumber for the CNT papers on glass slide (See Fig. A1-a. in Appendix).

According to the above results, it is evident that the wavenumbers of the three D, G and G' bands are dependent on the laser power/intensity used in the Raman measurement, even though the laser with a power of 10 mW is weak. Also, there exists the substrate effect on the Raman spectrum of the CNT papers. To have negligible effect of the laser power on the Raman spectrum of the CNT papers, we need to limit laser power to be less than or equal to 0.5 mW.

4. Discussion

It is known that both temperature and stress/strain can contribute the changes of the wavenumbers of the D, G and G' bands of CNTs. Most works reported the decrease of the wavenumbers

of the Raman peaks of CNTs with increasing temperature [12, 19–22], while some reported an opposite trend, i.e. increasing temperature leads to the increase of the wavenumbers of the Raman peaks of CNTs [23]. Such a different trend in the variations of the wavenumbers of the Raman peaks of CNTs with temperature is likely attributed to the contribution of the thermal expansion of CNTs, since the temperature dependence of the phonon frequency of crystal is represented by the anharmonic terms in the lattice potential energy, including anharmonic potential constants, occupation number of phonon, and thermal expansion of the crystal [24].

Similar to the temperature effect on the changes of the wavenumbers of the Raman peaks of CNTs, applying stress can lead to either the decrease of the wavenumbers of the Raman peaks of CNTs [25, 26] or the increase of the wavenumbers of the Raman peaks of CNTs [17, 27, 28]. The mechanisms for the opposite trends of the changes of the wavenumbers of the Raman peaks of CNTs under mechanical stress remain elusive. It might be due to the constraint of adjacent materials to the deformation of CNTs.

Assume that the CNT paper is initially at a stress-free state. Under thermal and mechanical loading, the wavenumbers of the Raman peaks of the CNT papers are dependent on temperature and deformation. For the CNT papers with thickness much less than the length and width, the stress state in the CNT papers can be treated as plane stress. There are only three strain components, ε_{xx} , ε_{xy} and ε_{xy} for the description of the strain state in the CNT papers, where ε_{xx} and ε_{yy} are the normal components and ε_{xy} is the shear component of the strain tensor. From the three strain components with $\varepsilon_{zz}\approx 0$ due to limited change in the thickness, we obtain volumetric strain, ε_{y} , and maximum shear strain, ε_{max} , as

$$\varepsilon_{V} = \varepsilon_{xx} + \varepsilon_{yy}$$
, and $\varepsilon_{max} = \frac{1}{2} \text{Max} \left[|\varepsilon_{xx} + \varepsilon_{yy} \pm \sqrt{(\varepsilon_{xx} - \varepsilon_{yy})^{2} + 4\varepsilon_{xy}^{2}}|, \sqrt{(\varepsilon_{xx} - \varepsilon_{yy})^{2} + 4\varepsilon_{xy}^{2}} \right]$ (1)

Therefore, the changes of the wavenumbers of the Raman peaks of the CNT papers under thermal and mechanical loading can be

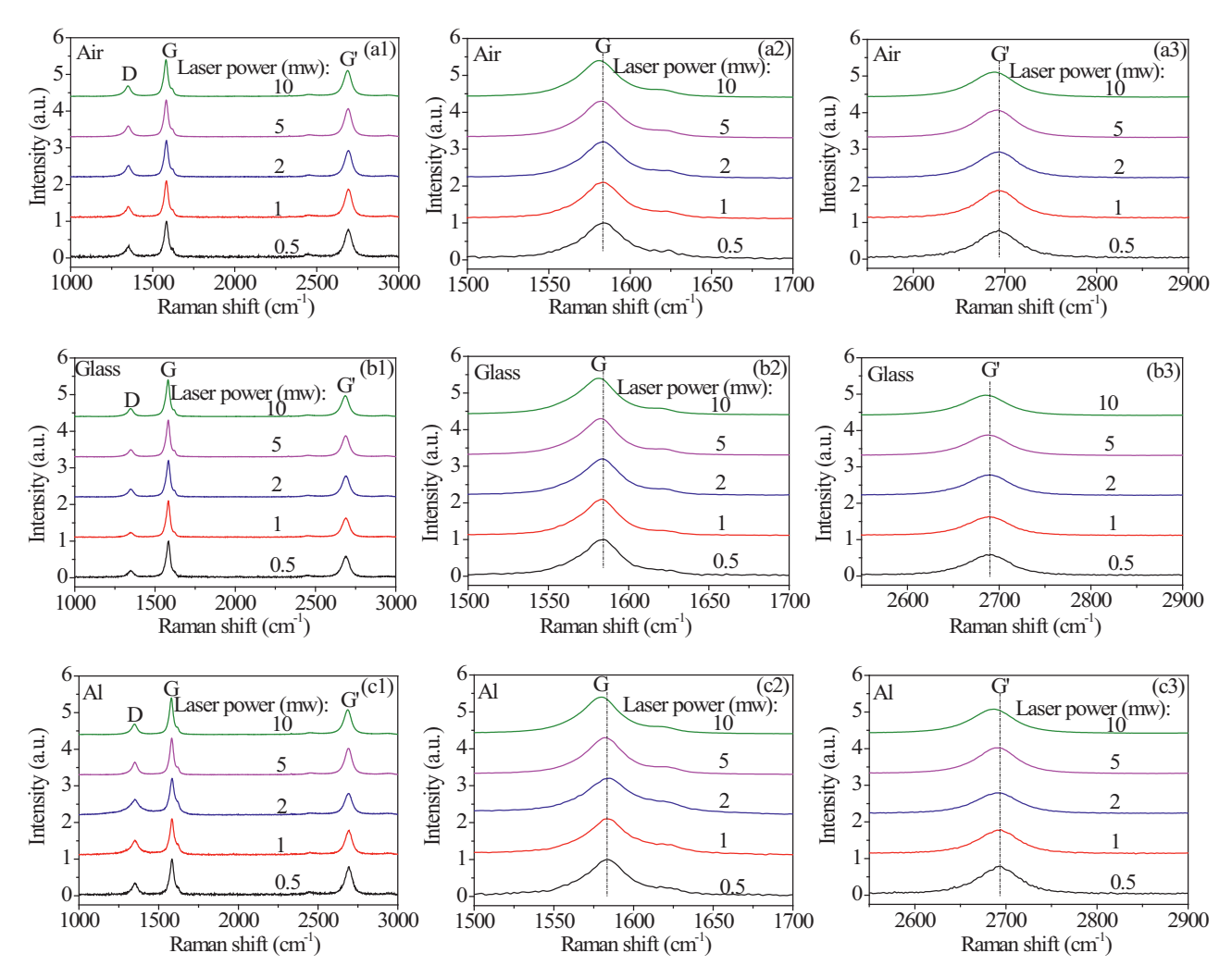


Fig. 4. Raman spectra of the CNT papers with and without solid substrate for different laser powers: (a) suspended CNT paper, (b) CNT paper on glass substrate, and (c) CNT paper on aluminum substrate.

expressed in the expansion of the Taylor series to the first order of the temperature change and the strains as

$$\Delta\omega_{i} = \alpha_{i}(T - T_{0}) + \beta_{i\nu}\varepsilon_{V} + \beta_{im}\varepsilon_{max}$$
 (2) with

$$\alpha_{i} = \frac{\partial \omega_{i}}{\partial T} \bigg|_{\varepsilon_{v} = 0, \varepsilon_{\text{max}} = 0, T = T_{0}}, \ \beta_{iv} = \frac{\partial \omega_{i}}{\partial \varepsilon_{v}} \bigg|_{\varepsilon_{v} = 0, \varepsilon_{\text{max}} = 0, T = T_{0}} \text{ and }$$

$$\beta_{im} = \frac{\partial \omega_{i}}{\partial \varepsilon_{\text{max}}} \bigg|_{\varepsilon_{v} = 0, \varepsilon_{\text{max}} = 0, T = T_{0}}$$
(3)

Here, ω is the wavenumber of the corresponding Raman peak of the CNT papers, T is absolute temperature, T_0 is the absolute temperature of the reference state, and the subscript, i, represents D, G or G' band. Eq. (2) provides the basis to analyze thermomechanical effects on the shifts of the Raman peaks of the CNT papers. Note that one needs to include higher-order terms in Eq. (2) for large change in temperature and large strains.

$$\Delta T = \frac{Pt}{coAI} \tag{4}$$

where c is the specific heat capacity of the CNT paper, ρ is the density of the CNT paper, and L is the thickness. Using the data available in literature, we have the specific heat capacity of the CNT papers as ~0.72 J/g·K at 300 K [29] and the density of the CNT papers as ~1.38 g/cm³ [30]. For P=10 mW, t=100 ns, and $A=9\pi/4~\mu m^2$ (the size of the laser beam is 3 μ m), the local temperature increase of the CNT paper is 178 K. This numerical value is compatible to the result reported by Li et al. [20]. Note that one can use Stokes and anti-Stokes Raman spectra to determine local temperature of materials from the ratio of corresponding peak intensities [31, 32]. Such an approach requires the acquirement of both the Stokes and anti-Stokes Raman spectra. Also, the calculation is based on the Boltzmann factor, which is likely dependent on the laser power used in the measurement.

Using the thermal expansion coefficient of CNTs, we approximate the thermal expansion coefficient of the CNT papers to be $2\times 10^{-5}~{\rm K}^{-1}$ [33]. For the laser spot of 3 $\mu{\rm m}$ in diameter, the increase in radius for the temperature increase of 178 K is 5.34 nm (1.78 \times 10⁻³ in strain). Such a small change in the radius of the laser-irradiated spot suggests that the thermal deformation of the CNT papers due to the laser irradiation can be treated as elastic, and the theory of linear thermoelasticity prevails.

According to the theory of linear thermoelasticity [34] and Appendix B, the strain components in the CNT papers are proportional to the temperature change with the proportionalities deter-

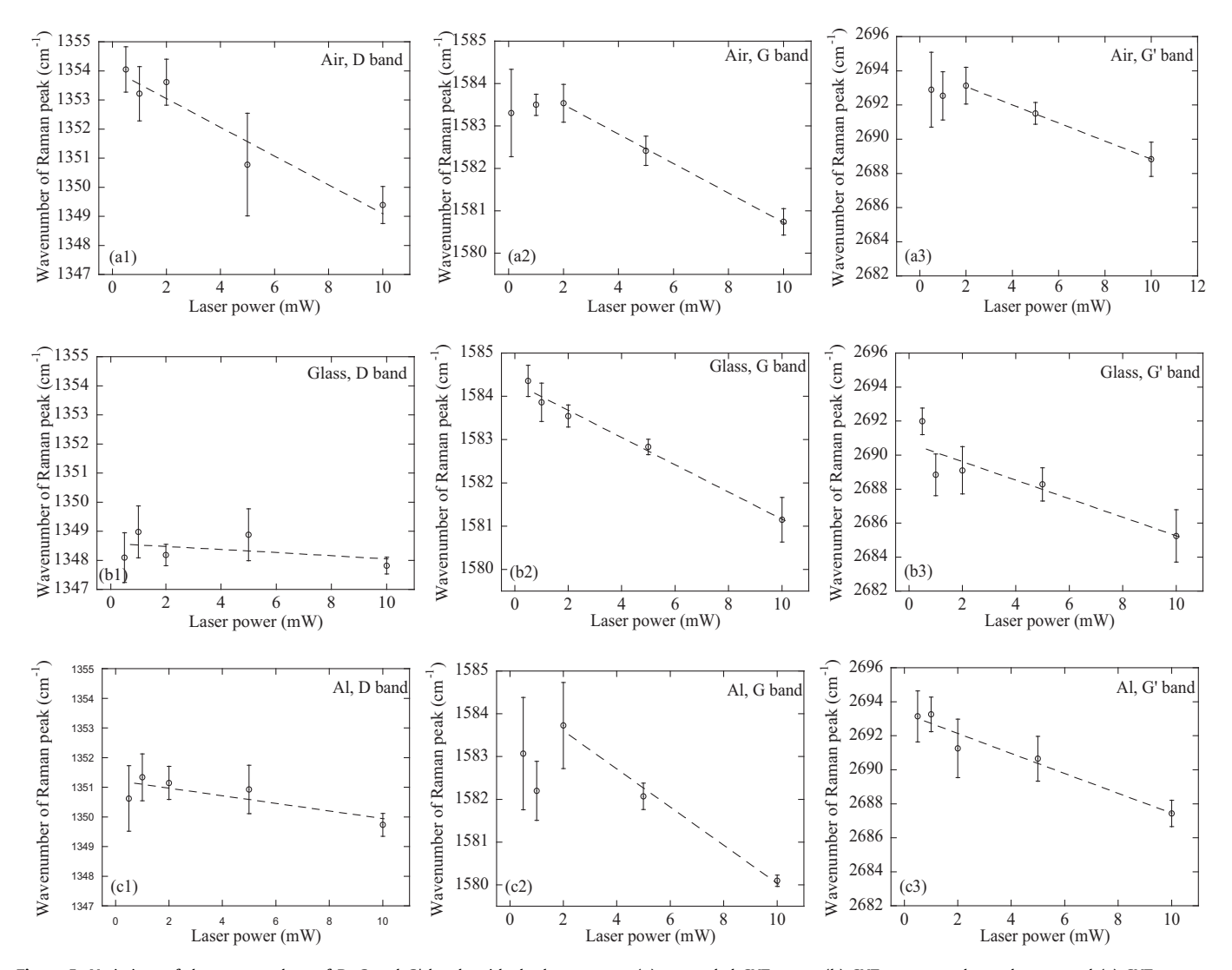


Figure 5. Variations of the wavenumbers of D, G and G' bands with the laser power: (a) suspended CNT paper, (b) CNT paper on glass substrate, and (c) CNT paper on aluminum substrate.

mined by the thermomechanical constants of the CNT papers and substrate and the geometrical constraints. Thus, we have $\varepsilon_V \propto (T-T_0)$ and $\varepsilon_{\rm max} \propto (T-T_0)$. Eq. (2) can be rewritten as

$$\Delta\omega_i = (\alpha_i + \chi_V \beta_{i\nu} \varepsilon_V + \chi_m \beta_{im})(T - T_0) \tag{6}$$

with χ_V and $\chi_{\rm m}$ as the corresponding proportionality constants, respectively. As discussed in Appendix B, the temperature increase of a thin film due to a laser irradiation is proportional to the laser power, i.e. $(T-T_0) \propto P$. Therefore, we have

$$\Delta\omega_i = \kappa (\alpha_i + \chi_V \beta_{iv} \varepsilon_V + \chi_m \beta_{im}) P \tag{7}$$

in which κ is a constant, depending on the thermal properties of the system, consisting of the CNT paper and surrounding material. It is evident that the thermomechanical properties of the surrounding material play an important role in the change of the Raman shift of the CNT papers. There exists thermomechanical coupling in determining the vibration of molecules under laser irradiation.

Table 1 lists the thermomechanical properties of the three materials of air, glass and aluminum at 25 °C. It is evident that there is a significant difference of thermal conductivities among the three materials, while there is a slight difference of thermal capacities. The differences in the thermomechanical properties lead to the difference in the thermomechanical responses of the

CNT papers to the laser heating during the Raman measurements, which likely results in the difference in the Raman shift shown in Figs. 5 and A1.

From Fig. 5, we note that there exists a range of the laser powers/intensities, in which the wavenumber of the corresponding Raman peak is proportional to the laser power. Using Eq. (7) to curve-fit the data in the corresponding range, we obtain the slope of $\Delta\omega_i/P$ for each case. For comparison, the fitting curves are included in Fig. 5. Fig. 6 shows the slopes of $\Delta \omega_i/P$ of the D, G and G' bands for the suspended CNT papers, the CNT papers on glass and the CNT papers on aluminum. It is evident that the slope of $\Delta \omega_i/P$ of the D band is significantly dependent on the abutting materials. The largest value of the slope of $\Delta\omega_i/P$ of the D band for the suspended CNT papers is likely attributed to the difference in the deformation state. The deformation of the suspended CNT papers due to the laser irradiation consists of global bending and local deformation associated with thermal expansion in contrast to the CNT papers on a "rigid" substrate which only experienced local deformation mainly associated with thermal expansion. Also, the slopes of $\Delta \omega_i/P$ of the D, G and G' bands for the CNT papers on the aluminum substrate are always larger than the corresponding ones for the CNT papers on the glass substrate. This trend reveals the possible effect of the thermal properties (thermal conductivity, thermal capacity and thermal expansion) of substrate on the

Table 1. Thermomechanical properties of air, glass and aluminum at 25 °C.

Material	Thermal conductivity $W/m \cdot K$	Thermal capacity J/kg·K	Thermal expansion coefficient, ${\rm K}^{-1}$	Elastic modulus GPa	Poisson' ratio
Air	0.02551	1007	N/A	N/A	N/A
Glass	0.8	800	$30-60 \times 10^{-7}$	70	0.23
Al	237	900	$21-24 \times 10^{-6}$	68	0.38

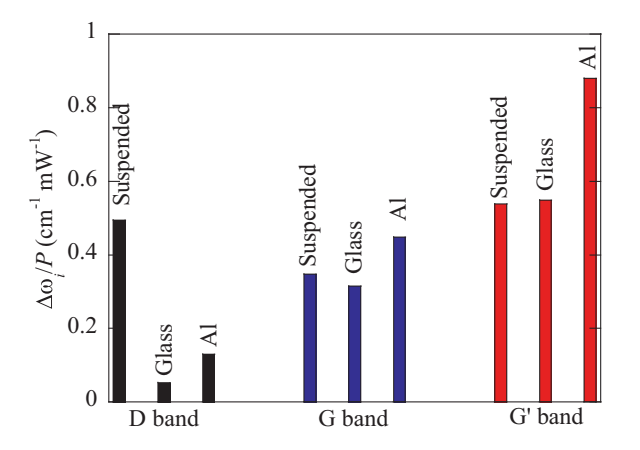


Fig. 6. Numerical values of $\Delta\omega_i/P$ of the CNT papers with and without solid substrates.

Table 2.Numerical values of the wavenumbers of the D, G and G' bands for the suspended CNT papers, the CNT papers on glass and the CNT papers on aluminum with the laser power of 0.5 mW.

Material	D band	G band	G' band
Air	1354.1±0.8	1583.3±1.0	2692.9 ± 2.2
Glass	1348.1±0.8	1584.4±0.4	2692.0 ± 0.8
Al	1350.6±1.1	1583.1±1.3	2693.1 ± 1.5

Raman shift of the CNT papers, since the numerical values of thermal conductivity, thermal capacity and thermal expansion of the aluminum substrate are larger than the corresponding ones of the glass substrate.

Table 2 lists the wavenumbers of the Raman peaks of the D, G and G' bands for the CNT papers with and without substrate for the Raman measurements with a laser power of 0.5 mW. It is evident that there are no statistical differences of the wavenumbers of the Raman peaks of the G and G' bands for the CNT papers with and without substrate. There are slight differences of the wavenumbers of the Raman peaks of the D band with and without substrate. These results together with the slopes of $\Delta \omega_i/P$ of the CNT papers with and without solid substrates, as shown in Fig. 6, suggest that a laser with a laser power equal to or less than 0.5 mW is needed if one wants to limit the combinational effects of abutting material and laser power on the Raman shift of the CNT papers,

5. Summary

The potential use of the Raman spectroscopy in the measurement of the deformation states in CNT-based and graphene-based materials has imposed a challenge on the understanding of the effects of abutting materials on the Raman spectrum of CNTs and graphene. We have investigated the Raman shifts of the CNT papers with and without the support of a solid substrate (glass and aluminum plates) for the Raman measurements with the laser power in a range of 0.5 to 10 mW. The experimental results reveal that there exist combinational effects of the abutting material

and laser power on the changes of the wavenumbers of the D, G and G' bands of the CNT papers.

For the suspended CNT papers, the laser irradiation with the power equal to or less than 2 mW has statistically no effect on the wavenumbers of all the three Raman peaks. The wavenumbers of all the three Raman peaks decrease with the increase of the laser power for the laser power in the range of 2 to 10 mW. For the CNT papers on the glass slide, the wavenumber for the D band is statistically independent of the laser power for the laser power in the range of 0.5 to 10 mW. Both the wavenumbers of the G and G' bands decrease with the increase of the laser power for the laser power in the range of 0.5 to 10 mW. For the CNT papers on the aluminum plate, the laser irradiation with the power equal to or less than 2 mW has statistically no effect on the wavenumbers of the D and G bands. The wavenumbers of both the D and G bands decrease with the increase of the laser power for the laser power in the range of 2 to 10 mW, and the wavenumber of the G' band decreases with the increase of the laser power for the laser power in the range of 0.5 to 10 mW.

Using the strain components, we have derived an analytical relation between the change of the wavenumber of a Raman peak, temperature and strains (volumetric strain and max shear strain) to the first order of the temperature change and the strains. In the framework of linear thermoelasticity, the change of the wavenumber of a Raman peak is proportional to the laser power, which is supported by the experimental results. We have performed linear-regression fitting of the experimental data. The fitting results reveal that there exists the possible effect of the thermal properties (thermal conductivity, thermal capacity and thermal expansion) of substrate on the Raman shift of the CNT papers.

Declaration of Competing Interest

The authors declare that they have no known competing financial interests or personal relationships that could have appeared to influence the work reported in this paper.

Acknowledgment

FY is grateful for the support by the NSF through the grant CMMI-1634540, monitored by Drs. Khershed Cooper and Thomas Francis Kuech, and CBET- 2018411 monitored by Dr. Nora F Savage. The authors thank Dr. Qingwen Li of Suzhou Institute of Nano-tech and Nano-bionics, Chinese Academy of Sciences, Suzhou for providing the CNT papers.

Appendix A

Fig. A1 shows the comparison of the wavenumbers of the D, G and G' bands of the CNT papers with and without the solid substrate under different laser powers. It is evident that the wavenumbers of the D, G and G' bands of the CNT papers are dependent on the substrate used to support the CNT papers.

Appendix B. Mathematical formulation of thermoelastic deformation of a CNT paper

Consider a thin circular plate of a in radius and h in thickness, which can be either suspended in air (Fig. 1a) or supported on a

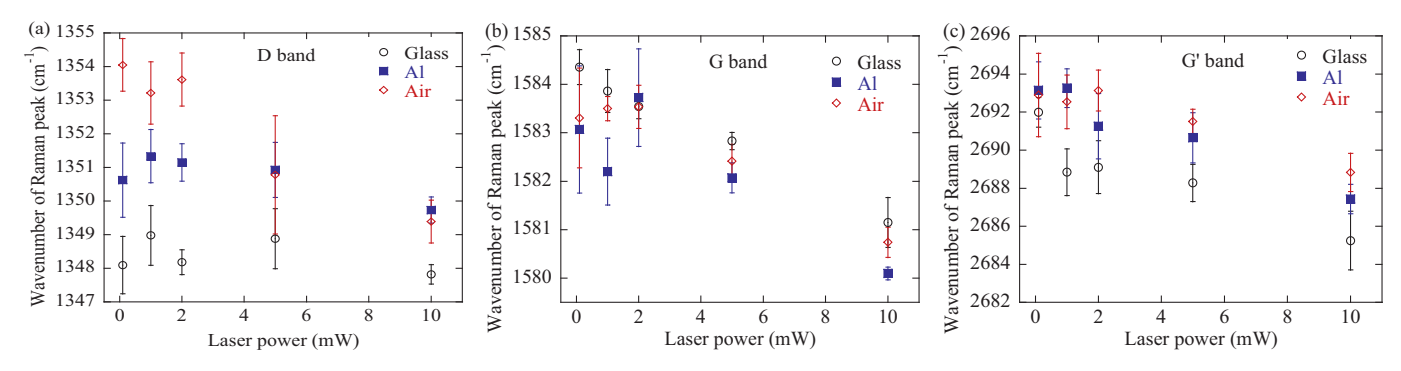


Fig. A1. Wavenumbers corresponding to Raman peaks in the Raman spectra of the CNT papers under different laser powers: (a) D band, (b) G band, and (c) G' band.

solid substrate (Fig. 1b). The thin circular plate experiences laser irradiation around the plate center for a period of t_0 . The laser power is P, and the area of the laser spot is A. The temperature of the thin circular plate prior to the laser irradiation is the same as the temperature of the surrounding materials.

The temperature evolution in the circular plate can be described by the following equation

$$\rho_1 c_1 \frac{\partial T_1}{\partial t} = k_1 \left(\frac{1}{r} \frac{\partial}{\partial r} \left(r \frac{\partial T_1}{\partial r} \right) + \frac{\partial^2 T_1}{\partial z^2} \right)$$
 (B1)

with initial condition and the boundary condition of top surface as

$$T_1(r, z, t)|_{t=0} = T_0$$
 (B2)

$$\left. \frac{\partial T_1(r,z,t)}{\partial z} \right|_{z=h} = \frac{\chi I(r)}{k_1} U(t_0 - t) \tag{B3}$$

For the suspended circular plate (Fig. 1a), the boundary condition of bottom surface is

$$k_1 \left. \frac{\partial T_1(r, z, t)}{\partial z} \right|_{z=0} = T_1 - T_0$$
(B4)

For the circular plate on a solid substrate (Fig. 1b), the heat conduction equation for the substrate is

$$\rho_2 c_2 \frac{\partial T_2}{\partial t} = k_2 \left(\frac{1}{r} \frac{\partial}{\partial r} \left(r \frac{\partial T_2}{\partial r} \right) + \frac{\partial^2 T_2}{\partial z^2} \right)$$
 (B5)

The boundary conditions at the interface between the circular plate and the substrate are

$$T_1(r, z, t)|_{z=0} = T_2(r, z, t)|_{z=0}$$
 and

$$k_1 \left. \frac{\partial T_1(r, z, t)}{\partial z} \right|_{z=0} = k_2 \left. \frac{\partial T_2(r, z, t)}{\partial z} \right|_{z=0}$$
(B6)

Here, ρ , c, k are the density, specific heat and thermal conductivity of the materials, respectively, χ is the fraction of the radiation energy absorbed into the circular plate per unit time and unit volume of the material, I(r) is the energy distribution of the laser beam, and $U(\bullet)$ is the step function. The subscripts 1 and 2 represent the circular plate and the substrate, respectively.

The relation between the laser intensity and the laser power is

$$I_0 = P/A = P/\pi R_s^2 \tag{B7}$$

with A and R_s as the area and radius of the laser spot on the top surface of the circular plate, respectively.

For small deformation and isotropic materials, the theory of linear thermoelasticity is applicable. The constitutive relations are

$$\boldsymbol{\varepsilon}_{i} = \frac{1}{2\mu_{i}} \left(\boldsymbol{\sigma}_{i} - \frac{\lambda_{i}}{2\mu_{i} + 3\lambda_{i}} tr(\boldsymbol{\sigma}) \mathbf{I} \right) + \alpha_{i} \Delta T_{i} \mathbf{I} (i = 1, 2)$$
 (B8)

The quasi-equilibrium equations are

$$\nabla \cdot \boldsymbol{\sigma}_i = 0 \tag{B9}$$

Here, μ and λ are the Lamé constants, and α is the coefficient of thermal expansion.

Assuming that the radiation pressure from the laser beam is negligible, we can approximate the top surface as a traction-free surface. For the suspended circular plate, the bottom surface is traction-free. For the circular plate on a solid substrate, the continuity of normal displacement component and normal stress prevail if there is no separation of the circular plate from the solid substrate.

According to Eqs. (B1)–(B9) and the linearity of the equations, we can conclude that the temperature changes and the stresses/strains are proportional to laser power of the laser beam irradiating to the top surface of the circular plate.

Eqs. (B1)–(B9) lay the foundation to solve the temporal evolution of temperature and stresses/strains in the circular plate for both the configurations in Fig. 1. However, it is generally very difficult to obtain analytical solutions of the thermomechanical problems. Numerical methods are generally needed for solving the thermomechanical problems.

References

- T. Dieing, O. Hollricher, J. Toporski, Confocal Raman Microscopy, Springer, New York, 2011
- [2] S. Ganesan, A. Maradudin, J. Oitmaa, A lattice theory of morphic effects in crystals of the diamond structure, Ann. Phys. 56 (1970) 556–594.
- [3] T. Wermelinger, R. Spolenak, Stress analysis by means of raman microscopy, in: Confocal Raman Microscopy, Springer, New York, 2010, pp. 259–278.
- [4] E. Liu, F. Conti, R. Signorini, E. Brugnolotto, S.K. Bhogaraju, G. Elger, in: Modelling Thermo-mechanical Stress in GaN-LEDs Soldered on Copper Substrate with Simulations Validated by Raman Experiments, EuroSimE, IEEE, 2019, pp. 1–8.
- [5] Y. Park, K. Hembram, R. Yoo, B. Jang, W. Lee, S.-G. Lee, J.-G. Kim, Y.-I. Kim, D.J. Moon, J.-K. Lee, Reinterpretation of single-wall carbon nanotubes by raman spectroscopy, J. Phys. Chem. C 123 (2019) 14003–14009.
- [6] E. Suslova, S. Chernyak, S. Maksimov, S. Savilov, Thermophysical features of carbon nanotubes frameworks formation by spark plasma sintering, Carbon 168 (2020) 597–605.
- [7] D. Casimir, H. Alghamdi, I.Y. Ahmed, R. Garcia-Sanchez, P. Misra, Raman spectroscopy of graphene, graphite and graphene nanoplatelets, in 2D Materials, Edited by C. Wongchoosuk and Y. Seekaew, IntechOpen, 2019, doi:10.5772/intechopen.84527.
- [8] K.-M. Hu, Z.-Y. Xue, Y.-Q. Liu, P.-H. Song, X.-H. Le, B. Peng, H. Yan, Z.-F. Di, J. Xie, L.-W. Lin, Probing built-in stress effect on the defect density of stretched monolayer graphene membranes, Carbon 152 (2019) 233–240.
- [9] K.L. Yang, J.O. Lee, H. Choo, F. Yang, Can Raman shift be used to characterize the mechanical property of graphene? J. Phys. Chem. C 122 (2018) 24467–24474.
- [10] K.R. Bagnall, E.A. Moore, S.C. Badescu, L. Zhang, E.N. Wang, Simultaneous measurement of temperature, stress, and electric field in GaN HEMTs with micro-Raman spectroscopy, Rev. Sci. Instrum. 88 (2017) 113111.
- [11] E. Tamdogan, G. Pavlidis, S. Graham, M. Arik, A comparative study on the junction temperature measurements of LEDs with raman spectroscopy, microinfrared (IR) imaging, and Forward voltage methods, IEEE Trans. Compon. Packag. Manuf. Technol. 8 (2018) 1914–1922.

[12] F. Huang, K.T. Yue, P. Tan, S.-L. Zhang, Z. Shi, X. Zhou, Z. Gu, Temperature dependence of the Raman spectra of carbon nanotubes, J. Appl. Phys. 84 (1998) 4022–4024

- [13] L. Zhang, H. Li, K.-T. Yue, S.-L. Zhang, X. Wu, J. Zi, Z. Shi, Z. Gu, Effects of intense laser irradiation on Raman intensity features of carbon nanotubes, Phys. Rev. B 65 (2002) 073401.
- [14] M. Steiner, M. Freitag, V. Perebeinos, J.C. Tsang, J.P. Small, M. Kinoshita, D. Yuan, J. Liu, P. Avouris, Phonon populations and electrical power dissipation in carbon nanotube transistors, Nat. Nanotechnol. 4 (2009) 320–324.
- [15] M. Sharma, S. Rani, D.K. Pathak, R. Bhatia, R. Kumar, I. Sameera, Manifestation of anharmonicities in terms of phonon modes' energy and lifetime in multiwall carbon nanotubes, Carbon 171 (2021) 568–574.
- [16] M. Steiner, M. Freitag, J.C. Tsang, V. Perebeinos, A.A. Bol, A.V. Failla, P. Avouris, How does the substrate affect the Raman and excited state spectra of a carbon nanotube? Appl. Phys. A 96 (2009) 271–282.
- [17] Q. Li, Y. Ge, X. Tan, Q. Yu, W. Qiu, Experiment research on deformation mechanism of CNT film material, J. Nanomater. 2016 (2016) 3942671.
- [18] J. Di, D. Hu, H. Chen, Z. Yong, M. Chen, Z. Feng, Y. Zhu, Q. Li, Ultrastrong, foldable, and highly conductive carbon nanotube film, ACS Nano 6 (2012) 5457–5464.
- [19] L. Ci, Z. Zhou, L. Song, X. Yan, D. Liu, H. Yuan, Y. Gao, J. Wang, L. Liu, W. Zhou, Temperature dependence of resonant Raman scattering in double-wall carbon nanotubes, Appl. Phys. Lett. 82 (2003) 3098–3100.
- [20] H. Li, K. Yue, Z. Lian, Y. Zhan, L. Zhou, S. Zhang, Z. Shi, Z. Gu, B. Liu, R. Yang, Temperature dependence of the Raman spectra of single-wall carbon nanotubes, Appl. Phys. Lett. 76 (2000) 2053–2055.
- [21] Q. Wu, Z. Wen, X. Zhang, L. Tian, M. He, Temperature dependence of G— mode in Raman spectra of metallic single-walled carbon nanotubes, J. Nanomater. 2018 (2018) 3410306.
- [22] Z. Zhou, X. Dou, L. Ci, L. Song, D. Liu, Y. Gao, J. Wang, L. Liu, W. Zhou, S. Xie, Temperature dependence of the Raman spectra of individual carbon nanotubes, J. Phys. Chem. B 110 (2006) 1206–1209.

- [23] N. Dilawar Sharma, J. Singh, A. Vijay, Temperature dependent Raman investigation of multiwall carbon nanotubes, J. Appl. Phys. 123 (2018) 155101.
- [24] E. Zouboulis, M. Grimsditch, Raman scattering in diamond up to 1900 K, Phys. Rev. B 43 (1991) 12490–12493.
- [25] M. Mu, S. Osswald, Y. Gogotsi, K.I. Winey, An in situ Raman spectroscopy study of stress transfer between carbon nanotubes and polymer, Nanotechnology 20 (2009) 335703.
- [26] A. Paipetis, Stress induced changes in the Raman spectrum of carbon nanostructures and their composites, in: Carbon Nanotube Enhanced Aerospace Composite Materials, Springer, New York, 2013, pp. 185–217.
- [27] E. Del Corro, J. González, M. Taravillo, E. Flahaut, V.n.G. Baonza, Raman spectra of double-wall carbon nanotubes under extreme uniaxial stress, Nano Lett. 8 (2008) 2215–2218.
- [28] C. Cooper, R. Young, M. Halsall, Investigation into the deformation of carbon nanotubes and their composites through the use of Raman spectroscopy, Composites Part A 32 (2001) 401–411.
- [29] N. Pradhan, H. Duan, J. Liang, G. Iannacchione, The specific heat and effective thermal conductivity of composites containing single-wall and multi-wall carbon nanotubes, Nanotechnology 20 (2009) 245705.
- [30] B. Han, X. Xue, Y. Xu, Z. Zhao, E. Guo, C. Liu, L. Luo, H. Hou, Preparation of carbon nanotube film with high alignment and elevated density, Carbon 122 (2017) 496–503.
- [31] B.J. Kip, R.J. Meier, Determination of the local temperature at a sample during Raman experiments using stokes and anti-stokes Raman bands, Appl. Spectrosc. 44 (1990) 707-711.
- [32] M.V. Balois, N. Hayazawa, F.C. Catalan, S. Kawata, T.-a. Yano, T. Hayashi, Tip-en-hanced THz Raman spectroscopy for local temperature determination at the nanoscale, Anal. Bioanal. Chem. 407 (2015) 8205–8213.
- [33] L. Deng, R.J. Young, I.A. Kinloch, R. Sun, G. Zhang, L. Noé, M. Monthioux, Co-efficient of thermal expansion of carbon nanotubes measured by Raman spectroscopy, Appl. Phys. Lett. 104 (2014) 051907.
- [34] A.E. Green, K.A. Lindsay, Thermoelasticity, J. Elast. 2 (1972) 1-7.